ResearchGate

See discussions, stats, and author profiles for this publication at: https://www.researchgate.net/publication/7164042

Temperature Profiles and Heat Dissipation in Capillary Electrophoresis

ARTICLE *in* ANALYTICAL CHEMISTRY · MAY 2006

Impact Factor: 5.64 · DOI: 10.1021/ac052075x · Source: PubMed

CITATIONS
23

READS
51

5 AUTHORS, INCLUDING:

Rosanne M Guijt
University of Tasmania
90 PUBLICATIONS **1,651** CITATIONS
SEE PROFILE

Miroslav (Mirek) Macka
University of Tasmania
215 PUBLICATIONS **4,015** CITATIONS
SEE PROFILE

Philip Marriott
Monash University (Australia)
310 PUBLICATIONS **6,853** CITATIONS
SEE PROFILE

Paul R Haddad
University of Tasmania
508 PUBLICATIONS **10,686** CITATIONS
SEE PROFILE

Available from: Miroslav (Mirek) Macka
Retrieved on: 28 January 2016

Anal. Chem. **2006,** *78,* 2684−2693

Temperature Profiles and Heat Dissipation in Capillary Electrophoresis

Christopher J. Evenhuis,† Rosanne M. Guijt,† Miroslav Macka,*,† Philip J. Marriott,‡ and Paul R. Haddad†

Australian Centre for Research on Separation Science (ACROSS), School of Chemistry, University of Tasmania, Private Bag 75, Hobart 7001, Tasmania, Australia, and School of Applied Science, RMIT University, RMIT City Campus, GPO Box 2476V Melbourne 3001, Victoria, Australia

While temperature control is usually employed in capillary electrophoresis (CE) to aid heat dissipation and provide acceptable precision, internal electrolyte temperatures are almost never measured. In principle, this limits the accuracy, repeatability, and method robustness. This work presents a fundamental study that combines the development of new equations characterizing temperature profiles in CE with a new method of temperature determination. New equations were derived from first principles relating the mean, axial, and inner wall electrolyte temperatures (T_{Mean}, T_{Axis}, T_{Wall}). T_{Mean} was shown to occur at a distance $1/\sqrt{3}$ times the internal radius of the capillary from the center of the capillary and to be a weighted average of $^2/_3T_{Axis}$ and $^1/_3T_{Wall}$. Conductance (G) and electroosmotic mobility (μ_{EOF}) can be used to determine T_{Mean} and T_{Wall}, respectively. Extrapolation of curves of μ_{EOF} versus power per unit length (P/L) at different temperatures was used to calibrate the variation of μ_{EOF} with temperature (T), free from Joule heating effects. μ_{EOF} increased at 2.22%/°C. The experimentally determined temperatures using μ_{EOF} agreed to within 0.2 °C with those determined using G. The accuracy of G measurements was confirmed independently by measuring the electrical conductivity (κ) of the bulk electrolyte over a range of temperatures and by calculating the variation of G with T from the Debye−Hückel−Onsager equation. T_{Mean} was found to be up to 20 °C higher than the external temperature under typical conditions using active air-cooling and a 74.0-μm-internal diameter (d_i) fused-silica capillary. A combination of experimentally determined and calculated temperatures enables a complete temperature profile for a fused-silica capillary to be drawn and the thickness of the stationary air layer to be determined. As an example, at $P/L = 1.00$ Wm^{-1}, the determined radial temperature difference across the electrolyte was 0.14 °C; the temperature difference across the fused-silica wall was 0.17 °C, across the poly(imide) coating was 0.13 °C, and across the stationary air layer was 2.33 °C.

Joule heating is an important factor to consider in electrodriven separations as it induces temperature changes in the electrolyte and thereby influences precision, accuracy, separation efficiency, and method robustness.[1−3] As the temperature of the electrolyte increases, the viscosity (η) and the electrical permittivity (ϵ) decrease.[4,5] At the same time, in fused-silica capillaries, there is an increase in the zeta potential (ζ) with temperature.[6,7] The rate of diffusion of analytes also increases with temperature. Radial temperature differences in the electrolyte lead to thermal peak broadening due to different electrophoretic mobilities at the central axis and near the inner wall of the capillary.[8−10] Grushka et al.[8] modeled the effects of capillary radius, electrical field strength, and buffer concentration on plate height and concluded that the radial temperature differences from Joule heating can have serious effects on separation efficiencies. Gobie and Ivory[10] described the positive feedback effect between conductivity and temperature known as the "autothermal effect". The increase of electrolyte conductivity with temperature results in greater currents and heat production and even greater temperatures. Hjerten[11] expressed the thermal zone deformation as the difference in the rates of electromigration of analytes at the center and near the wall of the capillary as a percentage of the axial velocity. Based on the decrease in viscosity that accompanies an increase in temperature, the thermal zone deformation is ~2.3%/°C of radial temperature difference. Grushka, Gobie and Ivory, and Hjerten independently concluded that the resulting velocity profile is expected to be parabolic rather than the flat profile typically described for capillary electrophoresis (CE).[12]

For the practising analytical chemist endeavoring to achieve optimal separations, a compromise is often required between using

* To whom correspondence should be addressed. Fax: +61-3-6226 2858. E-mail: mirek.macka@utas.edu.au.

† University of Tasmania.

‡ RMIT University.

(1) Lacey, M. E.; Webb, A. G.; Sweedler, J. V. *Anal. Chem.* **2002**, *74*, 4583−4587.

(2) Evenhuis, C. J.; Guijt, R. M.; Macka, M.; Marriott, P. J.; Haddad, P. R. *Electrophoresis* **2005**, *26*, 4333−4344.

(3) Rathore, A. S. *J. Chromatogr., A* **2004**, *1037*, 431−443.

(4) Atkins, P. W. *The Elements of Physical Chemistry*, 7th ed.; Oxford University Press: Oxford, 2001.

(5) Hamer, W. J. *Handbook of Chemistry and Physics*, 58th ed.; CRC Press: Cleveland, 1977.

(6) Kirby, B. J.; Hasselbrink, E. F. J. *Electrophoresis* **2004**, *25*, 187−202.

(7) Revil, A.; Glover, P. W. J.; Pezard, P. A. *J. Geophys. Res.* **1999**, *104*, 20021−20032.

(8) Grushka, E.; McCormick, J. R. M.; Kirkland, J. J. *Anal. Chem.* **1989**, *61*, 241−246.

(9) Luedtke, S.; Th., A.; von Doehren, N.; Unger, K. K. *J. Chromatogr., A* **2000**, *887*, 339−346.

(10) Gobie, W. A.; Ivory, C. F. *J. Chromatogr.* **1990**, *516*, 191−210.

(11) Hjerten, S. *Electrophoresis* **1990**, *11*, 665−690.

10.1021/ac052075x CCC: $33.50 © 2006 American Chemical Society
Published on Web 02/24/2006

the highest possible electrical field strength and the need to avoid excessive thermal peak broadening. Such broadening can be minimized by reducing the power dissipated per unit length (P/L), which can be monitored easily using measured values of current and voltage. A reduced P/L can be achieved first by employing the smallest internal diameter capillaries possible and second by using buffers with a low electrical conductivity. However, the latter strategy can result in electromigrational dispersion if there is a gross mismatch between the mobilities of the analytes and co-ions in the electrolyte.

During the past decade, a considerable amount of research has been conducted toward electrolyte temperature measurements in CE.[2,10,13−20] Burgi et al.[20] used the variation of μ_{EOF} and G that occurs with temperature to determine the internal temperatures of their capillaries. Their model assumed that any variation in μ_{EOF} was associated with changes to the viscosity of the electrolyte but did not take into account changes to the ϵ or ζ. At low power values, good agreement between the temperatures determined from their two methods was obtained, but at higher power levels, the temperatures differed significantly and it is expected that the temperatures obtained from measurements of electroosmotic mobility under these conditions would be unreliable. Knox and McCormack[21] used the variation in μ_{EOF}, electrical conductivity (κ), and electrophoretic mobility (μ) and assumed that the product $\epsilon\zeta$ was independent of temperature. Based on this model, the temperatures determined from the electroosmotic mobility and electrophoretic mobility were consistently higher than that based on electrical conductivity

A number of other methods have been employed to measure temperatures inside capillaries.[2,10,13−20] The most precise of these have involved additional instrumentation such as an NMR spectrometer,[17] which is not routinely applicable for use in commercial CE instruments. Alternative methods, such as the use of external thermocouples[10,13] or the use of bulk properties, have been limited to a precision of ≥1 °C.[14]

In previous work,[2] we introduced a simple method of determining the mean temperature of the electrolyte in the capillary (T_{Mean}) by measuring the average conductance (G). A linear relationship between G and the average power per unit length (P/L) was identified. Plots of G versus P/L were extrapolated to zero power to determine the conductance in the absence of Joule heating (G_0). The ratio of G to G_0 was used to find T_{Mean} at higher power levels. It was found that T_{Mean} increased linearly with P/L. Although the conductance method showed excellent precision (relative standard deviation (RSD) <1%), it is desirable to be able to confirm the accuracy of measurements of the electrolyte temperature using independent methods. Thermocouples have been used to measure external capillary temperatures,[10,13] but to place miniaturized temperature measurement devices inside CE capillaries to measure electrolyte temperatures without disturbing the system would be exceedingly difficult. In this paper, the electrolyte temperatures determined using electroosmotic mobility (μ_{EOF}) are compared with values obtained using conductance as a temperature probe. New equations are introduced to show the relationships between the temperature at the axis and near the inner wall of the capillary and T_{Mean}. An equation to locate the radial distance from the axis of the capillary where the mean temperature actually occurs is also introduced.

The aims of this work were to verify the temperature dependence of conductance using two independent methods, to use electroosmotic mobility free of Joule heating as a temperature probe and to compare the electrolyte temperatures obtained from G and μ_{EOF}. Furthermore, a method has been developed to determine the electrolyte temperatures both in the proximity of the inner wall of the capillary and also at its axis. This method would be suitable for routine use in commercial instruments and with a precision of better than 1 °C.

THEORY

The principles of Joule heating, power dissipation, and variation of conductance with temperature have been discussed thoroughly in the literature.[3,22,23] Only key equations to facilitate the present discussion and newly developed equations (eqs 6−9) are presented here.

Temperature Dependence of Conductance. The following section demonstrates how G can be used as a temperature probe to determine the mean temperature of the electrolyte in the capillary. Equations are presented to show how G varies with temperature including the contributions made from changes to the concentration, viscosity, dielectric constant, and stoichiometry of the electrolyte.

Conductance (G) is the inverse of resistance.[24] By applying Kohlrausch's law, the Debye−Hückel−Onsager (DHO) equation and Walden's rule, it is possible to calculate how G varies with temperature.[24,25]

$$G = \frac{1}{\eta}\left(\frac{cA}{L}\right)\left\{\eta\Lambda_0 - \left(\frac{z^2eF^2}{3\pi}\right)\left(\frac{2c}{\epsilon RT}\right)^{1/2} - q\eta\Lambda_0\left(\frac{z^3eF}{24\pi eRT}\right)\left(\frac{2c}{\epsilon RT}\right)^{1/2}\right\} \quad (1)$$

where η is the viscosity of the electrolyte, c is its molar concentration, A and L are the cross-sectional area and length of the capillary, respectively, Λ_0 is the specific conductivity at infinite dilution, z is the valency of the ions, e is the charge on an electron, F is Faraday's constant, R is the ideal gas constant, T is the absolute temperature, and q is a constant that depends on the stoichiometry of the electrolyte and the mobility of its ions.

(12) Jandik, P.; Bonn, G. K. *Capillary Electrophoresis of Small Molecules and Ions*, 1st ed.; VCH: New York, 1993.
(13) Nishikawa, T.; Kambara, H. *Electrophoresis* **1996**, *17*, 1115−1120.
(14) Liu, K.-L. K.; Davis, K. L.; Morris, M. D. *Anal. Chem.* **1994**, *66*, 3744−3750.
(15) Bello, M. S.; Righetti, P. G. *J. Chromatogr.* **1989**, *606*, 95−102.
(16) Bello, M. S.; Righetti, P. G. *J. Chromatogr.* **1989**, *606*, 103−111.
(17) Lacey, M. E.; Webb, A. G.; Sweedler, J. V. *Anal. Chem.* **2000**, *72*, 4991−4998.
(18) Thormann, W.; Zhang, C.-X.; Caslavska, J.; Gebauer, P.; Mosher, R. A. *Anal. Chem.* **1998**, *70*, 549−562.
(19) Berezovski, M.; Krylov, S. N. *Anal. Chem.* **2004**, *76*, 7114−7117.
(20) Burgi, D. S.; Salomon, K.; Chien, R.-L. *J. Liq. Chromatogr.* **1991**, *14*, 847−867.
(21) Knox, J. H.; McCormack, K. A. *Chromatographia* **1994**, *38*, 207−214.
(22) Petersen, N. J.; Nikolajsen, R. P. H.; Mogensen, K. B.; Kutter, J. P. *Electrophoresis* **2004**, *25*, 253−269.
(23) Kok, W. *Chromatographia* **2000**, *51* (Suppl.), S24−27.
(24) Atkins, P. W. *Physical Chemistry*, 7th ed.; Oxford University Press: Oxford, 2002.
(25) Horvath, A. L. *Handbook of Aqueous Electrolyte Solutions: Physical properties, estimation and correlation methods*, 1st ed.; Ellis Horwood Ltd.: Chichester, 1985.

(Details of calculating q are described in Chandra and Bagchi.[26]) It follows that conductance is inversely proportional to viscosity but also depends on the concentration of the electrolyte, its electrical permittivity, its absolute temperature, and whether it contains multivalent ions.

Viscosity decreases exponentially with increasing temperature,[24] and values for its variation with temperature for water[27] and for a range of electrolyte solutions[28] have been well documented. If the temperature increases from 25 to 65 °C, the viscosity of water or dilute aqueous electrolytes halves.[27,28] Over the same temperature range, the dielectric constant of water (ϵ_r) decreases linearly at a rate of ~0.46%/°C.[5,29]

Based on eq 1, and taking into account the variations of conductivity at infinite dilution, dielectric constant, and viscosity with temperature, the conductance of univalent 1:1 electrolytes is expected to increase at ~2.12%/°C.

Isono[28] determined experimentally the temperature coefficient of electrical conductivity (γ) for a wide range of electrolytes and found γ = 2.02%/°C for 1:1 electrolytes and 2.08%/°C for 2:1 electrolytes. At pH = pK_{a2}, the sodium phosphate buffer used in this experiment contained equal amounts of NaH_2PO_4 and Na_2HPO_4 (1:1 and 2:1 electrolytes). It is therefore reasonable to assume γ =2.05%/°C. Equation 2 allows the mean increase in temperature of the electrolyte (ΔT_{Mean}) to be determined,

$$\Delta T_{\text{Mean}} = \frac{G(T) - G_0}{\gamma} = \frac{G(T) - G_0}{0.0205} \qquad (2)$$

where $G(T)$ is the conductance that results from Joule heating and G_0 is the conductance extrapolated to zero power[2].

Temperature Dependence of Electroosmotic Mobility. Equation 3 shows that the electroosmotic mobility varies linearly with the product of the dielectric constant and ζ and inversely with viscosity.[12]

$$\mu_{\text{EOF}} = \frac{\nu_{\text{EOF}}}{E} = \frac{-\epsilon_r \epsilon_0 \zeta}{\eta} = \frac{-\epsilon \zeta}{\eta} \qquad (3)$$

The temperature dependence of ϵ and η have been well documented, but there are few experimental data on the variation of ζ with temperature.[6,7] It has been asserted by a number of authors that the product $\epsilon\zeta$ is temperature-independent,[21,22,30] but recently, it has been shown that, under the conditions used for this investigation, the product $\epsilon\zeta$ decreases with increasing temperature at a rate of ~0.07%/°C.[29]

Radial Temperature Gradients in Capillaries during CE. In this section, new equations are developed from first principles to demonstrate how the radial temperature difference depends on P/L and to show the interrelationships between T_{Mean} over the cross section of the capillary, T_{Wall} and T_{Axis}. (see Figure 1)

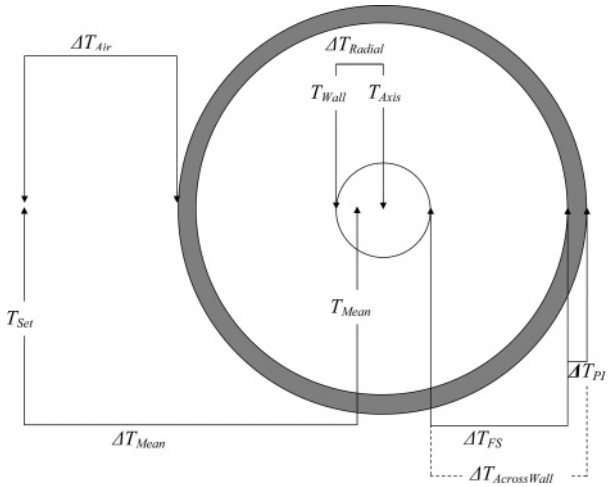

Figure 1. Schematic diagram showing the locations at which the temperature determinations are made.

The rate at which heat is dissipated in capillaries has been modelled by Knox[31] and independently by Jones and Grushka,[32] who suggested that a parabolic temperature profile would exist inside the capillary with a maximum along its central axis. Computer modeling by Bello and Righetti[16] showed that even if the electrolyte temperature increases by as much as 30 °C, the temperature profile is still essentially parabolic. This conclusion was supported by the Raman thermomicroscopic measurements made by Liu et al.[14] In a previous paper,[2] we have shown that the radial temperature difference can be calculated from first principles using the thermal conductivity of the electrolyte (λ) and P/L as described in eq 4,

$$\Delta T_{\text{Radial}} = T_{\text{Axis}} - T_{\text{Wall}} = \frac{VI}{4\pi\lambda L} = \frac{1}{4\pi\lambda}\frac{P}{L} \qquad (4)$$

where $\lambda \approx 0.605$ W m^{-1} K^{-1} for dilute aqueous electrolytes. Based on eq 4, the radial temperature difference is expected to increase linearly with the power per unit length at a rate of ~0.13 °C W^{-1} m.

A quadratic equation to model the parabolic temperature profile of the electrolyte inside the capillary is given in eq 5,

$$\Delta T(r) = (T_{\text{Axis}} - T_{\text{Wall}})\left(\frac{r_i^2 - r^2}{r_i^2}\right) \qquad (5)$$

where $\Delta T(r)$ is the difference in temperature between the inner wall and the electrolyte at a distance r from the central axis and r_i is the internal radius of the capillary. Integrating eq 5 for values of r between $-r_i$ and $+r_i$ and dividing the result by $2r_i$ leads to eq 6.

$$T_{\text{Mean}} - T_{\text{Wall}} = \frac{2}{3}(T_{\text{Axis}} - T_{\text{Wall}}) = \frac{2}{3}\Delta T_{\text{Radial}} \qquad (6)$$

Equation 6 can be rearranged to give eq 7 and used to determine

(26) Chandra, A.; Bagchi, B. *J. Chem. Phys.* **1999**, *110*, 10024−10034.
(27) NBS In *Handbook of Chemistry and Physics*, 58th ed.; Weast, R. C., Ed.; CRC Press: Cleveland, 1977; pp F51.
(28) Isono, T. *J. Chem. Eng. Data* **1984**, *29*, 45−52.
(29) Evenhuis, C. J.; Guijt, R. M.; Macka, M.; Marriott, P. J.; Haddad, P. R. *Electrophoresis* **2006**, *27*, 672−676.
(30) Hjerten, S. *Chromatogr. Rev.* **1967**, *9*, 122−219.
(31) Knox, J. H. *Chromatographia* **1988**, *26*, 329−337.
(32) Jones, A. E.; Grushka, E. *J. Chromatogr.* **1989**, *466*, 219−225.

T_{Wall} of the capillary when T_{Mean} and ΔT_{Radial} are known.

$$T_{Wall} = T_{Mean} - \frac{2}{3}\Delta T_{Radial} \quad (7)$$

Similarly, if T_{Mean} and ΔT_{Radial} are known, eq 8 can be used to find T_{Axis}.

$$T_{Axis} = T_{Mean} - \frac{1}{3}\Delta T_{Radial} \quad (8)$$

Thus, if the conductance and the radial temperature difference are known, it is possible to calculate the mean temperature of the electrolyte in the capillary and the electrolyte temperature near the inner wall and at the axis of the capillary.

The radial position (r_{Mean}) in the electrolyte for which $T = T_{Mean}$ can be found by solving eq 5 for $\Delta T(r) = {}^2/_3\ \Delta T_{Radial}$, which leads to eq 9,

$$\therefore\ r_{Mean} = \frac{r_i}{\sqrt{3}} \approx 0.58 r_i \quad (9)$$

where r_i is the internal radius of the capillary. This is in contrast to the relationship described by Porras et al.:[33] $r_{Mean} = 0.5 r_i$.

A schematic diagram showing the locations at which each of the temperatures is determined is shown in Figure 1.

EXPERIMENTAL SECTION

Apparatus. Experiments were performed on an HP^{3D} CE (Agilent, Palo Alto, CA) capillary electrophoresis instrument equipped with a UV absorbance detector using Chemstation software (Hewlett-Packard). The temperature of the vial tray was set to 25.0 °C using a Messegerate-Werk waterbath (Lauda, Königshofen, GDR). The internal temperature of the CE instrument where the sample vials were located during the run was monitored using a digital thermometer. A small fan powered by an external 12-V power supply was also introduced to circulate the air in this region.

Fused-silica capillaries with an internal diameter of 74.0 μm, an outer diameter of 362.8 μm, and a total length of 33.2 cm (Polymicro Industries Phoenix USA) were flushed with 0.1 M sodium hydroxide at a pressure of 95 kPa for 5 min before use. The external temperature of the capillary was set using the active cooling supplied by the CE instrument. The external diameters of the capillaries were measured using a digital electronic micrometer screw-gauge, Mitutoyo 601-906 (Takatsu-ku, Kawasaki, Japan). Measurements were made at 2-cm intervals along the length of the capillaries before averaging the results.

Chemicals. All solutions were prepared using Milli-Q (18 MΩ·cm) water. The buffer electrolyte (BGE) was prepared using AR grade orthophosphoric acid (BDH, Sydney, Australia) and AR grade sodium hydroxide (BDH). LR grade acetone (BDH) or LR grade thiourea (Ajax, Sydney, Australia) were used as neutral EOF markers. The 10 mM phosphate buffer (pH 7.21, ionic strength 22 mM) was produced by titrating 10.0 mM phosphoric acid solution with 12 M sodium hydroxide until the required pH was achieved. The EOF markers were produced by making a 20% solution by volume of acetone in the BGE or by adding thiourea to the BGE to a concentration of ~1 g L^{-1}.

Conductance Measurements. The current and voltage were monitored at intervals of 0.01 min throughout each run using the Chemstation software. Conductance values were calculated for each point in time up until the appearance of the EOF peak and were then averaged. The Agilent CE instrument's current and voltage readings were verified by connecting a 100-MΩ resistor in series with the electrodes and sweeping the voltage from 0 to 5 kV. The gradient of the voltage versus current plot was compared with the resistance of the 100-MΩ resistor.

EOF Measurements. Each capillary was flushed with the BGE (95.0 kPa) for 1 min before injecting the EOF marker at a pressure of 2.0 kPa for 3 s. Alternatively, an electrokinetic injection at 10 kV for 5 s was used. Measurements were made using separating voltages in increments of 5.0 kV with a total of five runs for each voltage. The EOF marker was detected using UV detection at 280 nm for acetone and at 250 nm for thiourea. Calculation of the electroosmotic mobility, μ_{EOF} was performed using eq 10,[34]

$$\mu_{EOF} = L_{tot}L_{det}/t_m V \quad (10)$$

where L_{tot} and L_{det} refer to the total length of the capillary (32.2 cm) and the length to the detector (23.7 cm), respectively, t_m is the migration time of the neutral marker, and V is the applied voltage.

Temperature Measurements. Voltage and current data were collected digitally using a commercial instrument at time intervals of 0.01 min and averaged over time until the EOF was detected. Electroosmotic mobility and conductance data were collected during the same run.

Conductance was calculated using the voltage and current data. G_0 was extrapolated from a plot of G versus P/L. The relationship expressed in eq 11 was used to find T_{Mean}.

$$T_{Mean} = 25.0\ °C + \frac{\{G_T/G_0 - 1\}}{0.0205\ °C^{-1}} \quad (11)$$

The accuracy of the thermal coefficient of electrical conductivity (γ) = 0.0205/°C was verified by calculating a theoretical value from first principles using the modified form of the DHO equation (eq 1) with the approximation for 1:1 electrolytes. Additionally, a conductivity cell calibrated with 0.010 00 M KCl using a Philips PW9504/00 resistance meter (North Ryde, NSW, Australia) was used to measure the variation of conductance with temperature for the phosphate electrolyte for a range of temperatures.

Similar to the approach described for conductance, the linear variation in the electroosmotic mobility was plotted as a function of the power per unit length and the value of μ_{EOF} at zero power dissipation (μ_{EOF}^0) was found by extrapolation. Two methods to find the internal temperature using the electroosmotic mobility were employed. The first method assumed that $\epsilon\zeta$ was constant so that the variation of μ_{EOF} with T was due only to changes in viscosity. μ_{EOF} was determined at different power levels with the

(33) Porras, S. P.; Marziali, E.; Gas, B.; Kenndler, E. *Electrophoresis* **2003**, *24*, 1553−1564.

(34) Jorgenson, J. W.; Lukacs, K. D. *Science* **1983**, *222*, 266−272.

external temperature set at 25 °C and was extrapolated to give the value at zero power. Mobilities at higher power levels were used to calculate the viscosity of the buffer using eq 12.

$$\eta(T) = \frac{\mu_{EOF}{}^{0}(25\ ^{\circ}C)}{\mu_{EOF}} \cdot \eta(25\ ^{\circ}C) \qquad (12)$$

In eq 12, $\eta(T)$ and $\eta(25\ ^{\circ}C)$ are the viscosities of the electrolyte at the elevated temperature as a result of Joule heating and at 25°C, respectively, and μ_{EOF} and $\mu_{EOF}{}^{0}(25\ ^{\circ}C)$ are the electroosmotic mobilities at the elevated temperature and for zero Joule heating at 25 °C, respectively. The temperature was calculated by interpolation using known values of viscosity.[27]

In the second method, the temperature was found by preparing a calibration curve for μ_{EOF} versus T, which would take into account any variations in $\epsilon\zeta$. The data for the calibration curve were obtained by setting the temperature of the cassette and vial tray to a particular value and measuring the variation of μ_{EOF} with P/L. The plot was extrapolated to zero power to give $\mu_{EOF}{}^{0}$ at that temperature. This procedure was carried out for a range of temperatures.

A correction factor was introduced to take into account the contribution from those parts of the capillary for which the temperature was measured but not controlled. For the capillary used, the effective temperature, $T_{Effective}$ of the electrolyte at zero power, was found using eq 13,

$$\text{length of nonregulated} = 6.6\ \text{cm} \rightarrow 20.5\%\ \text{of total}$$

$$\text{length of set temperature} = 25.6\ \text{cm} \rightarrow 79.5\%\ \text{of total}$$

$$T_{Effective} = 0.795T_{Set} + 0.205T_{Cavity} \qquad (13)$$

where T_{Set} is the set temperature in the actively cooled cassette and T_{Cavity} is the measured, but not controlled, temperature in the cavity of the instrument.

RESULTS AND DISCUSSION

The conductance of the electrolyte will determine the amount of heat produced.[2] Phosphate buffer (10.0 mM, pH 7.21) was chosen as a typical CE electrolyte. However, it is important to point out that the techniques presented here are equally applicable to other electrolytes having different conductivities. As the EOF markers were made up as dilute solutions in the BGE, it is safe to assume that any variation in plug lengths would have no effect on the measurement of μ_{EOF}.

Temperature Control. The precision of conductance and electroosmotic mobility values was improved by a factor of 5 by controlling the temperature of the vial tray by using a water bath to circulate water at a set temperature through the CE instrument. Nevertheless RSDs could not be reduced below 1%.

Porras et al.[33] pointed out that electrolyte temperatures measured using conductivities are significantly higher than those calculated from theoretical models. They attributed this discrepancy to almost half of their 30-cm capillary being outside the actively cooled cassette and in contact with still air. In this work, an attempt is made to quantify this effect. It was found that the temperature of the instrument cavity containing the parts of the capillary between the vials and the temperature-controlled cassette differed significantly from the set temperature (differences of up to 8 °C were observed). The capillary consists of five sections, which may have different temperatures, as illustrated in Figure 2. Two of these sections, of ~1.8 cm each, are in the vials containing the electrolyte, which had previously been set at the same temperature as the cassette using the waterbath external to the instrument. The heat loss in these sections would be more efficient than in the actively cooled cassette due to the large thermal conductivity of water and the absence of an insulating air layer.[2] Two more sections, ~3.3 cm each, are located between the vials and the cassette. Only passive cooling occurs in these sections since there is no means of controlling the temperature. The temperature in this region varies according to the room temperature and the temperature inside the instrument, which is influenced mainly by the period of time for which the lamp has been operating because of its large heat production. The fifth section is the part of the capillary in the cassette where the temperature external to the capillary is regulated.

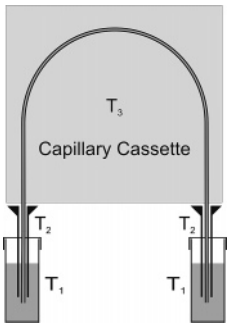

Figure 2. Schematic diagram of capillary showing variation of electrical conductivity for different parts.

Corresponding to the electrolyte temperatures in these sections, T_1, T_2, and T_3, are conductivities κ_1, κ_2, and κ_3. At low power levels, $\kappa_1 = \kappa_3 \neq \kappa_2$. At higher power levels, $\kappa_1 < \kappa_3 < \kappa_2$, reflecting the different abilities of the environmental surroundings of the capillary to dissipate heat. In the sections with temperatures T_1, T_2, and T_3, the respective cooling processes that occur are passive electrolyte cooling, passive air-cooling, and active air-cooling. The conductance measured by dividing the current by the voltage reflects an average value over the whole capillary, corresponding to the effective temperature, ($T_{Effective}$, see eq 13). As a result of the passive air-cooling that occurs in the cavity of the instrument, $T_{Effective}$ varied less than T_{Set}. Short capillaries were used in order to highlight radial temperature variations at high values of power per unit length, but these capillaries are also most prone to the influence of the axial differences in temperature and conductivity described above because the nonregulated parts comprise a larger fraction of the total length of the capillary than for longer capillaries.

At low voltages, the time taken for the EOF marker to be detected may exceed 30 min, allowing the temperature of the vials to change, especially if the set temperature is considerably different from the temperature of the cavity. It was found that the precision and accuracy were significantly higher in the shorter capillaries than in the longer capillaries.

Variation of Conductance and Electroosmotic Mobility with the Power Dissipated per Unit Length. G and μ_{EOF} showed

Table 1. Experimental Data[a]

V (kV)	I (μA)	P/L (W m^{-1})	G ($\times 10^{-9}$ S)	μ_{EOF} ($\times 10^{-9}$ m^2 s^{-1} V^{-1})	T_{Mean} (°C)[b]	T_{Wall} (EOF) (°C)[c]	$T_{Wall}(G)$ (°C)[d]	ΔT_{Radial} (°C)[e]	ΔT_{Radial} (°C)[f]
0.000	0.000	0.000	1.935	72.09	25.00	25.00	25.00	0.00	0.00
4.953	9.627	0.148	1.943	72.40	25.20	25.19	25.19	0.01	0.02
9.902	19.829	0.612	2.002	74.60	26.69	26.57	26.63	0.18	0.08
14.793	31.118	1.441	2.101	78.61	29.18	29.07	29.05	0.17	0.19
19.666	43.945	2.714	2.229	83.24	32.41	31.97	32.17	0.67	0.36
24.436	59.935	4.625	2.441	91.79	37.76	37.31	37.35	0.67	0.61
29.147	80.489	7.444	2.739	103.42	45.27	44.58	44.61	1.04	0.98

[a] Voltage (V), current (I), power per unit length (P/L), conductance (G), and electroosmotic mobility (μ_{EOF}). Mean temperature of electrolyte calculated from G (T_{Mean}), temperature of electrolyte near inside wall calculated from μ_{EOF} (T_{Wall}(EOF)), temperature of electrolyte near inside wall calculated from G ($T_{Wall}(G)$), radial temperature difference calculated from G and μ_{EOF} ($\Delta T_{Radial(Experimental)}$), and theoretical radial temperature difference calculated from first principles ($\Delta T_{Radial(Theoretical)}$). Conditions: 32.2-cm fused-silica capillary, d_i = 74.0 μm, d_o = 365 μm, BGE 10.0 mM phosphate buffer at pH 7.21, and set temperature 25.00 °C. EOF marker ~10 mM thiourea in BGE, electrokinetic injection 10 kV for 5.0 s. [b] $T_{Mean} = \{[G(T)/G(25\ °C)] - 1\}/0.0205 + 25\ °C$; eq 11. [c] $T_{Wall}(EOF) = \{[\mu_{EOF}/\mu_{EOF}{}^0(25\ °C)] - 1\}/0.0222 + 25\ °C$; eq 14. [d] $T_{Wall}(G) = T_{Mean} - {}^2/_3 0.1315\ P/L$; eq 7 and eq 4. [e] $\Delta T_{Radial(Experimental)} = {}^3/_2(T(G) - T(EOF)) = {}^3/_2(T_{Mean} - T_{Wall})$; eq 15. [f] $\Delta T_{Radial(Theoretical)} = P/(4\pi\lambda L)$; eq 4.

a linear dependence on P/L with observed R^2 values of 0.9996 and 0.9995, respectively. The measurements, 15 for each voltage, were averaged from data obtained over a number of days and are given in Table 1. Invariably, the conductivity data gave a higher degree of intraday reproducibility than the EOF data.

The temperatures determined from G and μ_{EOF} using eq 11 and eq 12 differed by up to 2.31 °C at P/L = 7.45 W m^{-1}, with μ_{EOF} yielding the higher temperature. This unexpectedly high value for the wall temperature originates from eq 12, which only takes into account changes to viscosity. A difference between the values determined from the two methods is expected since the EOF is generated near the wall and the associated temperature reflects the temperature of the buffer in proximity to the inner wall, T_{Wall}. On the other hand, the temperature calculated from the conductance data reflects the mean temperature of the electrolyte, T_{Mean}, which should be higher than T_{Wall} but smaller than T_{Axis}. The radial temperature difference is a result of the heat energy, which is conducted from the electrolyte to the actively cooled outside of the capillary and can be predicted by eq 4. The predicted value for ΔT_{Radial} at P/L=7.45 W m^{-1}, however, is 0.98 °C. The discrepancy of μ_{EOF} yielding higher temperatures than G is also apparent in the data obtained by Knox and McCormack[21] The resolution of this problem is discussed in Use of Electroosmotic Mobility as a Temperature Probe.

Use of Conductance as a Temperature Probe. Current and voltage measurements from the CE instrument were used to find the temperature dependence of conductance. This is simpler than the method described by Kok[23] as the internal diameter of the capillary is not required and G is much easier to calculate than κ. Plots of G versus P/L collected using different temperatures (see Figure 3 inset) were extrapolated to zero power dissipation to make a calibration curve free from the effects of Joule heating. These extrapolated values of G are shown as triangles and are plotted as a function of effective temperature (see Figure 3). The variation of conductance with temperature was calculated and verified from first principles using the modified DHO equation (eq 1). This equation contains several constant terms so that a good approximation for the variation of G with T can be obtained by considering variations in η and ϵ, for which values are tabulated. Substituting these values predicted γ = 2.12%/°C for 1:1 electrolytes (solid line in Figure 3).

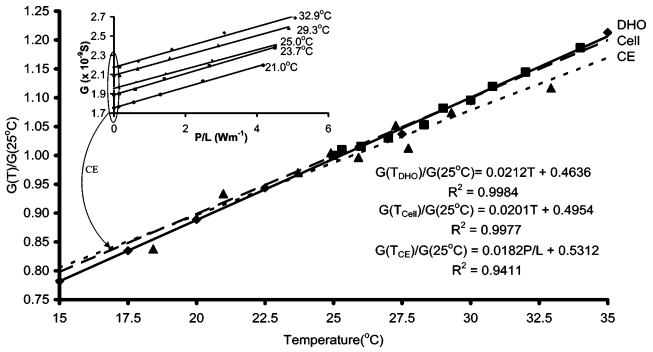

Figure 3. Variation of relative conductance with effective temperature (■) measurements from a conductivity cell and (▲) from the CE instrument using fused-silica capillaries (◆). Predictions from a modified DHO equation for a 1:1 electrolyte. Conditions: 32.2-cm fused-silica capillary, d_i. 74.0 μm, d_o. 362.8 μm, BGE 10.0 mM phosphate buffer at pH 7.21, EOF marker 20% v/v acetone in BGE, pressure injection 20 mbar for 3.0 s, range of effective temperatures 21.0−32.9 °C. Inset: Variation of conductance with the power dissipated per unit length. For clarity of the diagram, not all the lines used to produce the calibration graph for the CE instrument are shown.

At 25.0 °C, the conductance values for the 10 mM phosphate buffer pH 7.21 obtained from CE measurements were within 1% of those calculated from first principles for a 1:1 electrolyte. The conductivity of the phosphate electrolyte was also measured using a conductivity cell over a range of temperatures and plotted in Figure 3 (dashed line). The gradient obtained for the conductivity cell was 2.01%/°C, which is in good agreement with the 2.05%/°C used for the temperature calibration in eq 11.

Measurements of conductance using the CE instrument showed a smaller temperature dependence (1.82%/°C) than predicted from first principles. The lower gradient of the conductance curve from the CE measurements may be explained by the lack of temperature control in the cavity housing the vials during each run (see Temperature Control).

The variation of ΔT_{Mean} (determined from G using γ = 0.0205/°C) with P/L is plotted in Figure 4. ΔT_{Mean} was directly proportional to P/L and increased at a rate of 2.715 °C for each additional watt per meter of Joule heating.

Use of Electroosmotic Mobility as a Temperature Probe. The electroosmotic mobility observed at a particular power per

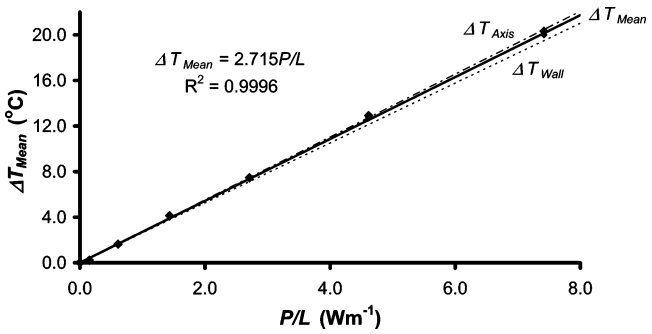

Figure 4. Variation of mean temperature increase, ΔT_{Mean} (measured by conductance), and calculated axial temperature, T_{Axis}, and wall temperature, T_{Wall}, with the power per unit length P/L. Conditions: As in Figure 3 but with a set temperature of 25.00 °C.

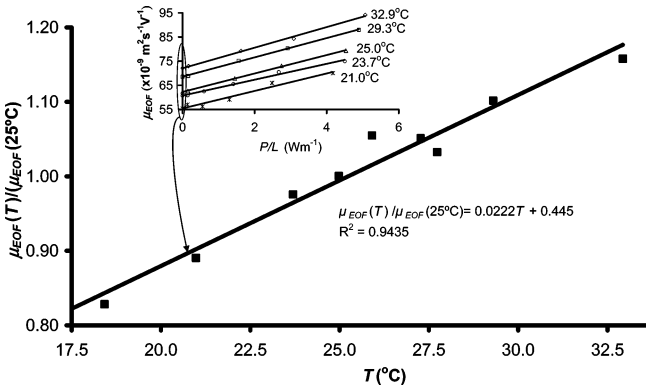

Figure 5. Variation of relative electroosmotic mobility, $\mu_{EOF}(T)/\mu_{EOF}(25\ °C)$ with effective temperature. Conditions: as in Figure 3 using EOF marker ~10 mM thiourea in BGE, electrokinetic injection 10 kV for 5.0 s. Inset: Variation of electroosmotic mobility, μ_{EOF} with the power dissipated per unit length, P/L for a range of effective temperatures from 21.0 to 32.9 °C. For clarity of the diagram, not all the lines used to produce the calibration graph are shown.

unit length was very sensitive to the room temperature and the temperature of the vial tray. To facilitate the use of μ_{EOF} as a temperature probe, it was important that the calibration curve for the variation of μ_{EOF} with T was free of the effects of Joule heating. The method presented here accomplished this by extrapolation to zero power rather than assuming minimal Joule heating effects at low power levels. In this study, the hypothesis is made that the temperature measured using μ_{EOF} is actually the temperature of the electrolyte near the inside surface of the capillary; which is where the electroosmotic flow is generated. To the best of our knowledge, this has not been reported previously.

The first method of using μ_{EOF} as a temperature probe assumed that the variation of μ_{EOF} with T was due only to changes in viscosity and led to the problems discussed in Variation of Conductance and Electroosmotic Mobility with the Power Dissipated per Unit Length. The second method of using μ_{EOF} as a temperature probe was a new approach, which allowed for variations in $\epsilon\zeta$ with temperature. In this method, μ_{EOF} was determined at different power levels for effective temperatures ranging from 21 to 33 °C and extrapolated to zero power. Plots of these data, shown in Figure 5 (inset), are essentially parallel, which suggests that the increase of the electrolyte temperature near the wall, T_{Wall}, is independent of the set temperature and depends only on the power per unit length. The extrapolated values of μ_{EOF} free from Joule heating at each effective temperature

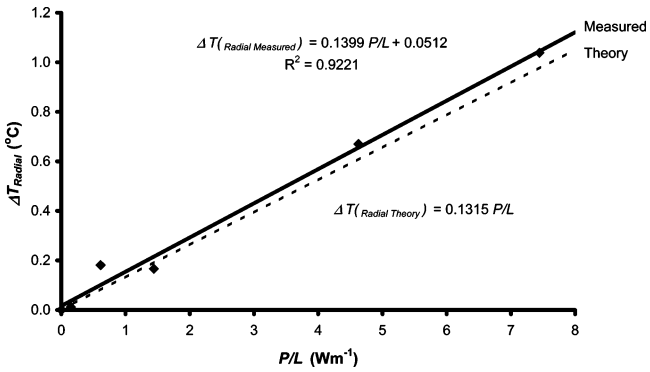

Figure 6. Radial temperature difference ($T_{Axis} - T_{Wall}$) calculated from first principles, $\Delta T_{(Radial\ Theory)}$ and $\Delta T_{(Radial\ Measured)}$ using conductance and electroosmotic mobility as temperature probes. Conditions: as in Figure 4.

were divided by the electroosmotic mobility free from Joule heating at 25 °C to find the relative electroosmotic mobility. The relative electroosmotic mobility was plotted as a function of the effective temperature to produce the calibration curve in Figure 5. The gradient of the least-squares line of best fit is 2.22%/°C enabling eq 14 to be used to determine T_{Wall} from measurements of μ_{EOF},

$$T_{Wall} = \frac{\{\mu_{EOF}/\mu_{EOF}{}^{0}(25\ °C)\}}{0.0222} + 25\ °C \qquad (14)$$

where μ_{EOF} is the electroosmotic mobility at the temperature to be determined and $\mu_{EOF}{}^{0}(25\ °C)$ is the electroosmotic mobility measured at 25 °C free of Joule heating. The temperatures of the electrolyte near the inner wall calculated from the electroosmotic mobility data and from the conductance data are shown in Table 1. In most cases, the values of T_{Wall} from the two independent methods agreed to within less than 0.1°C. The radial temperature difference can be calculated by rearranging eq 7 to produce eq 15.

$$\Delta T_{Radial} = \frac{3}{2}(T_{Mean} - T_{Wall}) \qquad (15)$$

Based on eq 4 using $\lambda = 0.605\ W\ m^{-1}\ K^{-1}$, a plot of ΔT_{Radial} versus P/L would be expected to have a gradient of $0.1315\ K\ W^{-1}\ m$. Using the experimentally obtained values for T_{Mean} and T_{Wall}, a measured gradient of $0.1399\ K\ W^{-1}\ m$ was found, which is in good agreement with the expected value (see Figure 6). Such close agreement between experiment and theory for T_{Wall} and ΔT_{Radial} would not be achieved using previously reported approaches.[7,20]

If one takes into account that μ_{EOF} is a measure of T_{Wall} and G is a measure of T_{Mean}, the apparent discrepancies in measurements of temperature obtained by Burgi et al.[20] and independently by Knox and McCormack[21] can now be understood. Their determinations of temperature did not take into account variations in the product $\epsilon\zeta$ when using μ_{EOF} as a temperature probe, nor was it recognized that G and μ_{EOF} act as temperature probes for the electrolyte at different radial locations in the capillary.

The radial temperature difference relates directly to the percentage zone broadening via differences in viscosity of the

electrolyte at the axis and near the inner wall of the capillary.[22] For temperatures close to 25 °C, the reciprocal of viscosity (and hence the velocity of an analyte) increases at 2.28%/°C.[29] It follows that if $P/L = 1.0$ W m^{-1}, $\Delta T_{Radial} = 0.13$ °C and the percentage zone broadening is 0.30%.

Temperature Profile of Fused-Silica Capillaries. Equations 11, 7, 8, and 4, developed in this work, were used to find T_{Mean}, T_{Wall}, T_{Axis}, and ΔT_{Radial}, respectively. Knox[31] showed that the temperature difference across the capillary wall ($\Delta T_{AcrossWall}$) depends on the rate at which heat is produced per unit volume of electrolyte (Q), the thermal conductivity of the wall (λ_{Wall}), and the inner and outer diameters of the capillary (d_i) and (d_o). This equation may be rearranged to produce eq 16, which shows that $\Delta T_{AcrossWall}$ depends linearly on P/L and is inversely proportional to λ_{Wall}.[2]

$$\Delta T_{AcrossWall} = \frac{1}{2\pi\lambda_{Wall}} \ln\left(\frac{d_o}{d_i}\right) \frac{P}{L} \quad (16)$$

It also shows that the thicker the capillary wall, the greater is $\Delta T_{AcrossWall}$.

For fused-silica capillaries, eq 16 can be applied to find both the temperature difference across the fused-silica wall (ΔT_{FS}) and across the poly(imide) coating (ΔT_{PI}). These two layers have very different thermal conductivities, 1.40 and 0.155 W m^{-1} K^{-1}, respectively.[13,31] The capillary used in this study had an internal diameter of 74.0 μm; the outer diameter of the fused silica was 321.0 μm and that of the poly(imide) coating was 362.8 μm. For $P/L = 1.00$ W m^{-1}, the temperature differences calculated using eq 16 are 0.167 °C for the fused silica and 0.126 °C for the poly(imide) coating. If these temperatures and the mean temperature of the electrolyte are known, it is possible to calculate the temperature difference across the static air layer using eq 17,

$$\Delta T_{Air} = \Delta T_{Mean} - 2/3\Delta T_{Radial} - \Delta T_{FS} - \Delta T_{PI} \quad (17)$$

where ΔT_{Mean} is the rise in the mean temperature of the electrolyte, ΔT_{Radial} is the temperature difference across the electrolyte, and ΔT_{FS} and ΔT_{PI} are the temperature differences across the fused silica and poly(imide), respectively (see Figure 1). Using the experimentally determined value of $\Delta T_{Mean} = 2.71$ °C at $P/L = 1.00$ W m^{-1}, eq 17 gives $\Delta T_{Air} = 2.33$ °C. By rearranging eq 16, an estimate for the thickness of this static air layer can be made by assuming it acts as a hollow cylinder with inner dimensions equal to the outer diameter of the capillary. Equation 18 may be used to calculate the thickness of the static air layer (x_{Air}),

$$x_{Air} = \frac{1}{2} d_o (e^{(2\pi\lambda_{Air}\Delta T_{Air}/P/L)} - 1) \quad (18)$$

where $\lambda_{Air} = 0.025$ W m^{-1} K^{-1} is the thermal conductivity of the air[31] and the other symbols have their usual meaning. Substituting into eq 18 predicts an air layer thickness (x_{Air}) of ~80 μm at 1.00 W m^{-1}. This simple model also confirms what one would expect intuitively, that x_{Air} is independent of the rate of Joule heating. One can come to the same conclusion by rearranging Newton's law of cooling to give eq 19,[22,35]

$$\Delta T_{Air} = \frac{x_{Air}}{\pi d_o \lambda_{Air}} \frac{P}{L} = \frac{1}{\pi d_o h} \frac{P}{L} \quad (19)$$

where h is the heat-transfer coefficient.. Clearly x_{Air} would depend on the efficiency of the cooling system. Rearrangement of eq 18 and substituting $x_{Air} = 80.4$ μm gives $h = 312$ W m^{-2} K^{-1}. When checking the literature values for h using Peltier air cooling, Petersen et al. reported values of h in the range 11−114 W m^{-2} K^{-1} and Bello and Righetti reported a value of 240 W m^{-2} K^{-1} for an air-cooled Beckman instrument. This suggests that the value of 312 W m^{-2} K^{-1} is not unreasonable for the Agilent instrument.

A complete temperature profile for the capillary at 1.00 W m^{-1} is shown in Figure 7. At higher power levels, each of the temperature differences shown will be correspondingly larger.

CONCLUSIONS

While internal electrolyte temperatures are almost never measured in CE, some control of temperature is usually employed, with the assumption that the difference between the set temperature and the actual electrolyte temperature that results from Joule heating is insignificant. However, as found in this work, at typical operating conditions, the temperature changes of the electrolyte in the capillary often reach tens of degrees. This has great significance for the accuracy, repeatability, and efficiency of electromigrational separations. The method presented here has enabled temperature changes occurring in commercial instruments to be quantified accurately and easily. A method developed previously by this group for measuring the mean temperature of the bulk electrolyte based on conductance and a new method that determines the temperature of the electrolyte near the inner wall of the capillary based on electroosmotic mobility are capable of determining these temperatures with an accuracy of 0.2 °C.

Unlike conductance, which is a fairly rugged temperature probe, the electroosmotic mobility is well known to be sensitive to many parameters, including changes to the surface charge and surface properties, electrolyte composition, and the presence of impurities. Therefore, in principle, it cannot be expected that EOF measurement will be a generally robust temperature probe.

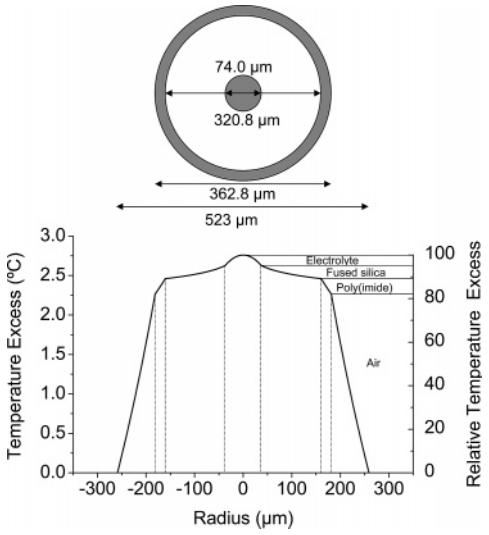

Figure 7. Schematic diagram showing the temperature profile for a fused-silica capillary. Conditions: as in Figure 4 with $P/L = 1.00$ W m^{-1}.

Table 2. Glossary of Terms

abbreviation	quantity	unit
ΔT_{Air}	temperature difference across air layer surrounding capillary (see Figure 1)	°C
$\Delta T_{AcrossWall}$	temperature difference across the capillary wall (sum of ΔT_{FS} and ΔT_{PI} (see Figure 1)	°C
ΔT_{Axis}	change of electrolyte temperature at capillary axis as a result of Joule heating	°C
ΔT_{FS}	temperature difference across fused-silica wall (see Figure 1)	°C
ΔT_{Mean}	change in mean temperature of the electrolyte as a result of Joule heating (see Figure 1)	°C
ΔT_{PI}	temperature difference across poly(imide) coating (see Figure 1)	°C
ΔT_{Radial}	radial temperature difference across electrolyte (see Figure 1)	°C
$\Delta T(r)$	temperature difference between electrolyte and the inner wall of the capillary at a distance r from the axis	°C
ΔT_{Wall}	change of electrolyte temperature near capillary wall as a result of Joule heating	°C
ϵ	electrical permittivity of electrolyte	F m^{-1}
ϵ_0	electrical permittivity of a vacuum	8.8542×10^{-12} F m^{-1}
ϵ_r	dielectric constant of water	dimensionless
ζ	zeta potential	V
η	viscosity of electrolyte	kg m^{-1} s^{-1}
κ	electrical conductivity of electrolyte	S m^{-1}
λ	thermal conductivity of electrolyte	W m^{-1} K^{-1}
λ_{Air}	thermal conductivity of air	W m^{-1} K^{-1}
λ_{FS}	thermal conductivity of fused silica	W m^{-1} K^{-1}
λ_{PI}	thermal conductivity of poly(imide)	W m^{-1} K^{-1}
λ_{Wall}	thermal conductivity of wall	W m^{-1} K^{-1}
μ_{EOF}	electroosmotic mobility	m^2 s^{-1} V^{-1}
$\mu_{EOF}{}^0$	electroosmotic mobility free from Joule heating	m^2 s^{-1} V^{-1}
$\mu_{EOF}{}^0$(25 °C)	electroosmotic mobility free from Joule heating at 25°C	m^2 s^{-1} V^{-1}
c	molar concentration	mol L^{-1}
d_i	internal diameter of capillary	m
d_o	external diameter of capillary	m
E	electrical field strength	V m^{-1}
EOF	electroosmotic flow	
F	Faraday's constant	96487 Cmol^{-1}
G	conductance	S
h	heat-transfer coefficient	Wm^{-2}K^{-1}
I	electric current	A
L_{det}	length of the capillary to the detector	m
L_{tot}	total length of the capillary	m
P/L	power per unit length	W m^{-1}
Q	rate of heat production per unit volume	W m^{-3}
r	distance from the axis of the capillary	m
r_i	internal radius of capillary	m
r_{Mean}	distance from axis to the location where $T = T_{Mean}$	m
R	Ideal gas constant	8.3144 J mol^{-1} K^{-1}
t_m	time for EOF marker to migrate to the detector	s
T	temperature or absolute temperature	°C or K
T_{Axis}	temperature of the electrolyte at axis of capillary (see Figure 1)	°C
T_{Cavity}	temperature measured in the cavity of the instrument	°C
$T_{Effective}$	effective temperature of the electrolyte without Joule heating	°C
T_{Mean}	mean temperature of the electrolyte in the capillary (see Figure 1)	°C
T_{Set}	set temperature of air used for active cooling of cassette (see Figure 1)	°C
T_{Wall}	temperature of the electrolyte near the inner wall of capillary (see Figure 1)	°C
T_{Wall}(EOF)	temperature of the electrolyte near the inner wall of capillary determined using electroosmotic mobility	°C
$T_{Wall}(G)$	temperature of the electrolyte near the inner wall of capillary determined using conductance	°C
v_{EOF}	velocity of the electroosmotic flow	m s^{-1}
V	applied voltage	V
x_{Air}	thickness of stationary air layer surrounding capillary	m

Another factor making μ_{EOF} unsuitable as a routine temperature probe is the need for a separate calibration curve for the variation of μ_{EOF} with temperature for each electrolyte as the gradient of the curve will vary. This time-consuming process is necessary as the electroosmotic mobility is affected by variations in ζ and ϵ, and electrolyte composition, not just η as was previously assumed.

Nevertheless, in this work, a new method has been introduced to use μ_{EOF} as a temperature probe in order to validate the previously introduced method of temperature measurement based on conductance. The new method has demonstrated that, if sufficient experimental care is exercised, temperatures can be determined accurately using measurements of either EOF or conductance.

Newly developed equations interrelate the electrolyte temperatures T_{Axis} with T_{Wall} and T_{Mean}: T_{Mean} is a weighted average of $^2/_3T_{Axis}$ and $^1/_3T_{Wall}$ and occurs at a distance $r_i/\sqrt{3}$ from the central axis not at $r_i/2$ as previously reported. All three temperatures can be determined experimentally from either G or μ_{EOF} data. The values obtained from these two independent methods generally agreed to within 0.1 °C. The experimentally determined radial temperature differences agreed to within 0.1 °C with those

(35) Hutchings, R. *Physics*, 1st ed.; Macmillan Education Ltd.: London, 1990.

calculated from first principles using the thermal conductivity of the electrolyte.

Radial temperature differences are a major cause of zone broadening. Equation 4 developed in this work provides a simple means of predicting that the radial temperature difference is ~0.13 °C at 1.0 W m^{-1}. Based on the change of viscosity, the associated zone broadening is then 0.30%. Therefore, thermally induced zone broadening can be predicted simply by monitoring P/L and multiplying the measurement by 0.3%. The temperature differences across the fused-silica wall and poly(imide) coating can also be calculated as a function of P/L and show that the thin poly(imide) layer contributes 43% of the temperature difference between the inner and outer walls. Using a novel equation based on the interrelationships between T_{Mean} and T_{Wall}, a complete temperature profile was obtained for an actively air-cooled fused-silica capillary. Unlike the previously published semiquantitative profile, this profile is on a quantitative scale and includes the thickness of the static air layer. The example shown of a standard polyimide-coated fused-silica capillary illustrates that over 80% of the total rise in temperature occurs across the static air layer. Obviously, to minimize the rise in temperature of the electrolyte, those components made of materials having low thermal conductivity have to be minimized. Therefore, in the first place, the air layer surrounding the capillary should be excluded wherever possible by the use of a liquid coolant or by direct contact with a heat sink. Smaller improvements could also be achieved by using thinner coatings of poly(imide). Obviously the exact shape of a particular temperature profile will reflect the experimental parameters including the electrical conductivity of the electrolyte, the capillary material and dimensions and the efficiency of the cooling system.

In future work, the methods presented here will be used as a basis for computer modeling of temperature increases during electrodriven separations and to acquire electrophoretic mobility values that are unaffected by Joule heating. It is anticipated that the methods presented in this work will be generally applicable, even to electrodriven processes in different electrolyte systems and in microfluidic devices.

ACKNOWLEDGMENT

The authors thank Mr. John Davis for his assistance in calibration of the CE instrument and Dr. Michael Breadmore for helpful discussions. Funding from the Australian Research Council is gratefully acknowledged. R.M.G. also acknowledges financial support from the Dutch Foundation of Science and Technology STW (project DPC 6168).

Received for review November 24, 2005. Accepted January 30, 2006.

AC052075X